Effects of Breathing and Breath-hold on Brain Functional Connectivity

Anusha A S
Dept. of EE, IISc
Bengaluru, India
anushas@iisc.ac.in

A G Ramakrishnan
Dept. of EE, IISc
Bengaluru, India
agr@iisc.ac.in

Adarsh A
Dept. of EE, IISc
Bengaluru, India
adarsha@iisc.ac.in

Kanishka Sharma
Dept. of EE, IISc
Bengaluru, India
kanishkas@iisc.ac.in

G Pradeep Kumar
Dept. of EE, IISc
Bengaluru, India
pradeepkg@iisc.ac.in

***Abstract*—Recent years have seen a wealth of literature increasingly recognizing the concept that breathing rhythms entrain the activity of the human brain. However, the mechanisms underlying this phenomenon, and the extent to which rhythmic brain activity is modulated by breathing are not fully understood at the moment. The study reported herein is a preliminary step towards that goal. The variations in the electroencephalogram (EEG) based functional connectivity (FC) of the human brain during normal breathing, and voluntary breath-hold has been investigated and reported here. An experimental protocol involving breathing and breath-hold sessions, synchronized to a visual-metronome was designed and administered on 20 healthy subjects (9 females and 11 males within a range of 23-60 years). EEG data were collected from all subjects during breathing and breath-hold sessions using the 64 channel eego^{TM}mylab system from ANT Neuro. Further, FC was estimated on brain hemispheres and 7 cortical regions for 5 specific EEG bands, and variations were examined statistically. The observations illustrated that the brain FC exhibits a hemispherical symmetry during breath-hold in the delta and alpha bands. Synchronization of neuronal assemblies in different cortical regions of the brain was found to be higher in low-frequency EEG bands and lower in high-frequency EEG bands. Furthermore, the study also revealed that gamma-band FC of the pre-frontal cortex could distinctly identify an inhale-hold from exhale-hold.**

***Index Terms*—Functional connectivity, phase synchronization, EEG, breathing, breath-hold**

I. Introduction

Breathing is one of the most basic functions of the human body. It allows the body to obtain the energy it needs to sustain itself . Breathing happens naturally at rest and involves automatic but active inspiration and passive expiration [1]. Each breath is known to follow a rhythm, triggered and synchronized by coupled oscillators driving the respiratory cycle, most prominently the preBötzinger complex located in the medulla [2]. This brainstem neural microcircuit controls respiration autonomously, making the act of breathing seem effortless and continuous even during sleep or when a person is unconscious. However, it is also possible for humans to voluntarily control their breathing, during speech, singing, crying, or during voluntary breath-holding. Even though this adaptive characteristic of respiration can be an indication of the top-down architecture of the functional neuroanatomy of voluntary respiratory control [3], the mechanisms underlying breath control, and the extent to which rhythmic brain activity is modulated by the rhythmic act of breathing is not fully understood at the moment.

While a wealth of literature has focussed on the physiology [4]–[6] and the neurophysiology of breathing [7], mainly investigating the automatic breathing driven by brainstem structures, recent years have seen the cortical involvement, and higher brain mechanisms underlying the cognitive aspects of breathing, gaining more research interest [8]. Animal studies have conclusively shown the respiration-driven entrainment of neural activity in different cortical regions, including those involved in sensory responsiveness and higher cognitive functions such as the olfactory cortex [9], whisker barrel cortex [10], and associative neocortical regions [11].

While these animal studies highlight the widespread impact of respiration on brain functioning and its relevance in different cognitive processes, these links are not yet critically investigated in humans. Limited but relevant exceptions to this include a recent study by Perl et al. [12], which investigated the hypothesis that olfactory stimulus acquisition is perfectly synchronized with inhalation, which tunes neuronal ensembles for incoming information. The authors observed that mental processes like visuospatial perception are phase-locked with nasal inhalation, consistent with the notion of an olfaction-based template in the evolution of the human brain function. Similarly, evidence for respiratory entrainment of local field potential activity in the human piriform cortex, amygdala, and hippocampus was observed by C. Zelano et al. [13], in intracranial electroencephalogram (iEEG) data obtained from epileptic patients.

Breath control in the form of voluntary breath-hold has also been investigated to understand the coupling between neural and respiratory dynamics. As voluntary breath-hold tasks can induce arterial hypercapnia (increase in arterial CO_2 level), it has been widely used to evaluate the effects of variations in CO_2 levels in human subjects [14]. Such tasks, however, can only be administered in an adult population, while more sophisticated techniques like end-tidal capnography or depth camera system are used for quantitative evaluation of respiration in children and neonates [15], [16]. Recent studies by Morelli et al. [17], [18] explored the cross-correlation between EEG global field power (GFP) in delta band and end-tidal CO_2 during 30 seconds of breath-hold. They observed that

the variation of $P_{ET}CO_2$ precedes the variations of GFP. They also reported a generic coupling between delta EEG power and $P_{ET}CO_2$ and a pure nonlinear interaction between alpha EEG power and $P_{ET}CO_2$, suggesting that during hypercapnic inhalation, brain activity resembles a low arousal state. Recent studies on the synchronization of the cardiovascular system and respiration from our group have reported for the very first time that respiration-inspired fluctuations in the heart rate persists during breath-hold intervals too [19], [20].

In animals, on the other hand, the effect of hypercapnia on brain activity has been explored by gas administration. Hypercapnia was found to reduce the spontaneous neuronal oscillatory power in anesthetized primates [21] and rats [22], and, if prolonged (8 weeks), caused hypnotic effects without changing the morphological aspect of the brain in rabbits [23]. Thus, both animal and human studies give preliminary indications of the pivotal role of nasal breathing and breath-hold in coordinating neuronal oscillations associated with rest or cognition.

However, further comprehensive investigations are warranted to identify the extent to which breathing and breath-hold modulate rhythmic brain oscillations at rest or during a cognitive task, to locate the cortical regions where the modulations are localized, and to distinguish the effects during different phases of the respiratory cycle. The study reported herein is a primary step to this end. This study aims to investigate the differences in the electroencephalogram (EEG) based functional connectivity (FC) of the human brain during normal breathing, and voluntary breath-hold. Hemispheric FC variations, as well as FC variations in different cortical regions of the brain, are analyzed and the observations are reported here.

A. Brain Functional Connectivity

Brain functional connectivity analyses have become an increasingly important tool for revealing fundamental elements of human brain architecture and organization, in recent years [24]. Functional connectivity (FC) is fundamentally a statistical concept that captures statistical relations between distributed and spatially remote units within a nervous system. These units can be individual neurons, neuronal assemblies/populations, or anatomically segregated brain regions. Functional relations are investigated and established either during cognitive tasks or perceptual tasks or even when a subject is at rest. Nonetheless, the underlying objective of all these investigations is to study how neurons and neural networks process information. FC analyses are based on the hypothesis that different tasks or even resting-state require a well-coordinated flow of information between different functionally specialized brain areas as defined based on the functional specialization theory in neuroscience [25].

FC is often calculated between all elements of a system, regardless of whether these elements are structurally linked. It is highly time-dependent and statistical patterns between neuronal assemblies fluctuate on multiple time scales, some as short as tens or hundreds of milliseconds [26]. It is also worth noting that FC does not make any explicit reference to an underlying structural framework or specific directional effects.

II. Study Objectives

The study reported herein is envisaged as a precursor to further investigations concerning the effect of different breathing techniques and rhythms on the FC patterns of the human brain. This study investigates the following aspects associated with normal breathing and breath-hold conditions: (i) Whether any hemisphere-specific EEG-based FC variations exist between normal breathing and breath-hold conditions, and (ii) Whether different cortical regions of the brain respond differently, in terms of the EEG-based FC, during normal breathing and breath-hold conditions.

The variations are analyzed separately for 5 specific EEG bands viz., Delta (0.5-4 Hz), Theta (4-8 Hz), Alpha (8-12Hz), Beta (12-30 Hz), and Gamma (30-80 Hz).

III. Methodology

A. Subject Characteristics

20 subjects (9 females and 11 males) participated in the study. The age range of participants was 23-60 years, with a median age of 30.5 years (interquartile range: 10.3 years). All of them were right-handed, in self-reported good health with no signs or history of any acute/chronic respiratory pathologies. Participation in the study was voluntary and based on the understanding that observations would be published. Written informed consent was obtained from all participants.

B. Hardware description

EEG data were acquired from all subjects using the eego^{TM}mylab system from ANT Neuro. The system constitutes a 64 + 8 channel eego amplifier with a sampling rate of 16 kHz and Waveguard™ EEG cap with a 64 channel IFCN extended 10-10 standard electrode layout. Conductive clear gel was used to maintain the scalp-electrode impedance within the acceptable 5-20 kΩ range. Fig. 1 illustrates the EEG electrode placement. Data were recorded at a sampling frequency of 1 kHz.

C. Study Protocol

All subjects were instructed to take a shampoo head bath and to avoid oil on hair, hair spray, and metal accessories while coming for data recording. Upon arrival at the data collection venue, the subject was briefed about the study protocol, and the written consent was collected.

During the entire duration of the protocol, the subject sits upright and relaxed. The protocol involved three phases viz., baseline (BL), when the subject breathes normally for a duration of 5 minutes followed by a prolonged inhale hold (PRIH) phase and prolonged exhale hold (PREH) phase, each for a duration of 2 minutes. The breathing rate was maintained at 2 cycles per minute for the PRIH and PREH phases. During the PRIH phase, the subject inhales for 7.5 seconds, holds the breath for the following 15 seconds, and then exhales for 7.5

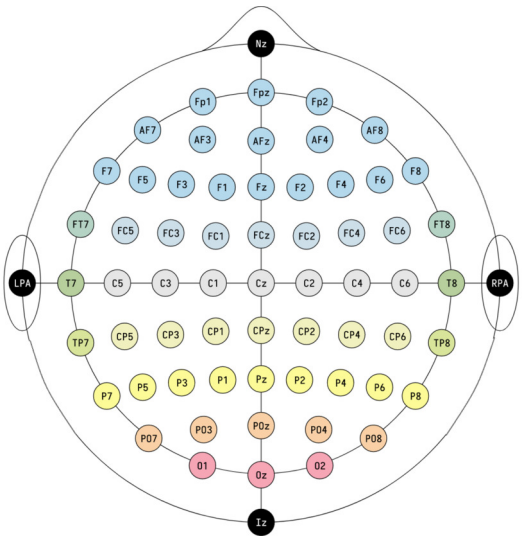

Fig. 1. EEG electrode positions in the 10-10 system. Each electrode placement site has a letter to identify the lobe, or area of the brain: pre-frontal (Fp), anterior frontal (AF), frontal (F), fronto-central (FC), temporal (T), central (C), temporo-parietal (TP), centro-parietal (CP), parietal (P), parieto-occipital (PO), and occipital (O). A "z" refers to an electrode placed on the midline sagittal plane of the skull. Nz denotes the nasion which is the distinctly depressed area between the eyes, just above the bridge of the nose, and Iz is the inion, which is the crest point of back of the skull. LPA and RPA denote the left and right pre-auricular points.

s. This cycle is repeated for a 2-minute duration. Similarly, during the PREH phase, the subject inhales for 7.5 seconds, exhales for the following 7.5 seconds, and then holds breath for 15 seconds.

A visual metronome was designed and developed in-house to help the subjects synchronize their breathing during PRIH and PREH phases. The metronome has two concentric circles. The blue inner circle slowly growing in diameter from the centre, to reach the boundary of the outer circle depicts inspiration. Similarly, the inner circle contracting from the boundary of the outer circle to the centre depicts expiration. The subject has to fix his gaze at the center and synchronize his breathing to the metronome. Also, when the circle is static, the subject holds the breath. Since a uniform inhale and exhale duration is desired across different subjects, breath-holds of equal intervals were added both after inhalation and exhalation. The metronome is uploaded on our lab website and is available for public access of fellow researchers [27]. The study protocol was approved by the Institute Human Ethics Committee (IHEC) of the Indian Institute of Science (IHEC No: 16/20200821).

D. Data Pre-processing

All pre-processing was done using EEGLAB version 13.4 - an interactive MATLAB toolbox for processing continuous and event-related EEG and other electrophysiological data [28].

EEG data collected from each participant during BL, PRIH, and PREH phases were subjected to line noise removal using the CleanLine EEGLAB plugin. This plugin adaptively estimates and removes line noise from EEG channels using multi-tapering and a Thompson F-statistic. EEG epochs of 2.5s duration were generated from BL, PRIH, and PREH phases. While the entire duration of baseline data was used to generate normal breathing (NB) epochs, the breath-hold segments from PRIH and PREH phases were respectively used to generate inhale-hold (IH), and exhale-hold (EH) epochs. The SIFT EEGLAB plugin was used to perform a piecewise detrending on the data to remove any trends. Further, the independent component analysis (ICA) using the runica algorithm was performed to remove artifacts embedded in the data without removing the affected data portions. The clean EEG data, thus generated, were used for further analyses.

E. Functional Connectivity Estimation

FC between all possible pairs of EEG electrodes was estimated by assessing the stability of phase difference between the corresponding time series, precisely called the phase synchronization measurement. Mathematically, phase synchronization is defined as follows:

Let $\boldsymbol{X}_{jt}$ and $\boldsymbol{Y}_{jt}$ be two multivariate time series, for discrete time $t = 0, 1.....N_T - 1$, with $j = 1, 2, ...N_R$ denoting the j-th analysis segment. Let $\boldsymbol{X}_{jk}$ and $\boldsymbol{Y}_{jk}$ indicate discrete Fourier transforms of these multivariate time series that contain both phase and amplitude information, for discrete frequencies $k = 0, 1.....N_T - 1$.

The phase synchronization between these two multivariate time series is defined as:

$$\phi^2_{X,Y}(k) = 1 - \frac{\left|\begin{pmatrix} \boldsymbol{S}_{\hat{\boldsymbol{Y}}\hat{\boldsymbol{Y}}\boldsymbol{k}} & \boldsymbol{S}_{\hat{\boldsymbol{Y}}\hat{\boldsymbol{X}}\boldsymbol{k}} \\ \boldsymbol{S}_{\hat{\boldsymbol{X}}\hat{\boldsymbol{Y}}\boldsymbol{k}} & \boldsymbol{S}_{\hat{\boldsymbol{X}}\hat{\boldsymbol{X}}\boldsymbol{k}} \end{pmatrix}\right|}{\left|\begin{pmatrix} \boldsymbol{S}_{\hat{\boldsymbol{Y}}\hat{\boldsymbol{Y}}\boldsymbol{k}} & \boldsymbol{0} \\ \boldsymbol{0}^{\boldsymbol{T}} & \boldsymbol{S}_{\hat{\boldsymbol{X}}\hat{\boldsymbol{X}}\boldsymbol{k}} \end{pmatrix}\right|} \tag{1}$$

where $\boldsymbol{S}_{\hat{\boldsymbol{Y}}\hat{\boldsymbol{Y}}\boldsymbol{k}}$, $\boldsymbol{S}_{\hat{\boldsymbol{Y}}\hat{\boldsymbol{X}}\boldsymbol{k}}$, $\boldsymbol{S}_{\hat{\boldsymbol{X}}\hat{\boldsymbol{Y}}\boldsymbol{k}}$, and $\boldsymbol{S}_{\hat{\boldsymbol{X}}\hat{\boldsymbol{X}}\boldsymbol{k}}$ are the corresponding covariance matrices that contain the phase information with amplitude factored out by normalization, and $\boldsymbol{0}$ denotes a matrix of zeros.

In the case that the two time series are univariate, then phase synchronization can be defined as:

$$\phi^2_{X,Y}(k) = \left|\frac{1}{N_R}\sum_{j=1}^{N_R} \hat{\boldsymbol{x}_{jk}}\hat{\boldsymbol{y}_{jk}}^*\right|^2 \tag{2}$$

In both cases, the measure is non-negative and takes a zero value only when there is independence of pertinent type.

FC computations were done for 5 specific EEG bands as mentioned in section II. In line with study objectives, FC computations were done separately for the left (LH) and right (RH) brain hemispheres as well as for seven brain cortical regions. The cortical regions considered were pre-frontal (pF), anterior frontal (AF), frontal (F), central (C), temporal (T), parietal (P), and occipital (O). Table 1 summarizes the EEG electrodes considered for the hemisphere-based and cortical region-based FC analyses.

F. Statistical Analyses

The Wilcoxon signed-rank test at a significance level of 0.05 was performed to determine whether any statistically significant differences existed between the functional connectivity of

TABLE I
BRAIN REGIONS AND CORRESPONDNG EEG ELECTRODES CONSIDERED FOR FUNCTINAL CONNECTIVITY ANALYSES

Region	Electrodes	# Electrodes	# Connections
Left brain hemisphere (LH)	Fp1, AF3, AF7, F1, F3, F5, F7, FC1, FC3, FC5, FT7, C1, C3, C5, T7, CP1, CP3, CP5, TP7, P1, P3, P5, P7, PO3, PO7, O1	26	325
Right brain hemisphere (RH)	Fp2, AF4, AF8, F2, F4, F6, F8, FC2, FC4, FC6, FT8, C2, C4, C6, T8, CP2, CP4, CP6, TP8, P2, P4, P6, P8, PO4, PO8, O2	26	325
Pre-frontal (pF)	Fp1, Fpz, Fp2	3	3
Anterior frontal (AF)	AF7, AF3, AFAF4, AF8	5	10
Frontal (F)	F7, F5, F3, F1, Fz, F2, F4, F6, F8	9	36
Central (C)	C5, C3, C1, Cz, C2, C4, C6	7	21
Temporal (T)	FT7, FT8, T7, T8, TP7, TP8	6	15
Parietal (P)	P7, P5, P3, P1, Pz, P2, P4, P6, P8	9	36
Occipital (O)	O1, Oz, O2	3	3

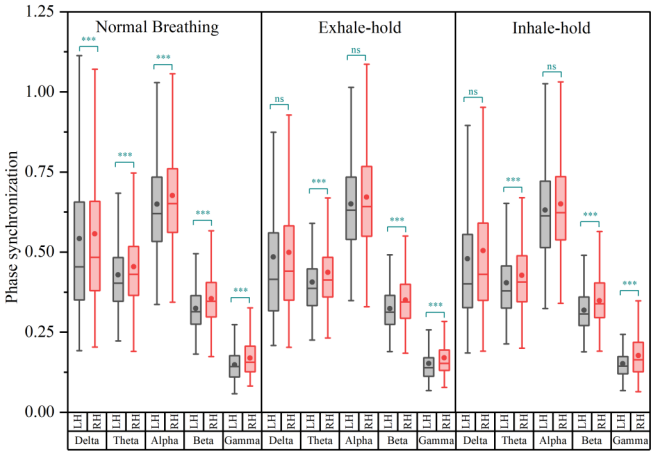

Fig. 2. Grand average of FC estimations in the left and right brain hemispheres. Box is determined by the 25th and 75th percentiles. Whiskers indicate 1.5 times the interquartile range (IQR). Circle represents the mean value and dash represents the median value. Representation of significance thershold is as follows: ns is $p > 0.05$, * is $p \leq 0.05$, ** is $p \leq 0.01$, and *** is $p \leq 0.001$.

the left and right brain hemispheres during the three conditions viz., normal breathing (NB), Exhale-hold (EH), and Inhale-hold (IH). Further, differences in the functional connectivity measures among the three groups across different cortical regions of the brain were compared by the Friedman's analysis of variance (ANOVA). The threshold for significance was set at $p<0.05$. When statistically significant effects were observed, post hoc tests were performed to evaluate the between-group variation with multiple comparison correction. Tests were done separately for each EEG band. Furthermore, the Pearson and Spearman correlations were computed between the functional connectivity measures of brain hemispheres as well as all possible pairs of cortical regions.

IV. Results and Discussions

As discussed in section III.E, FC (in terms of phase synchronization) in the left and right brain hemispheres were estimated during NB, EH, and IH. Estimations were done separately for 5 specific EEG bands. Fig. 2 summarizes the grand average of these computations involving 325 functional connections in each hemisphere, over all epochs from all subjects.

As can be seen, the average FC is comparatively higher in the lower frequency bands (viz., delta, theta, and alpha) than in the higher frequency bands (viz., beta, and gamma) for all three cases, in both hemispheres. These dynamics can be the reflection of the fact that while high-frequency brain waves are normally associated with complex neuronal tasks, low-frequency brain waves are associated with the control of vital functions, such as respiration and hemodynamics [18].

It is also evident from Fig. 2, that during normal breathing, the brain exhibits a hemispheric asymmetry, indicated by statistically significant differences between the FC in the left and right brain hemispheres, across all bands. And the connectivity is significantly higher in the right hemisphere than in the left. Studies have suggested that an overall control of the rhythmic nasal cycle occurs at the level of the hypothalamus of the brain [29]. Thus, electrical pulses originating from the hypothalamus generates a rhythmic nasal cycle, which will stimulate the brainstem oscillators symmetrically; but these oscillators influence nasal airflow asymmetrically due to their reciprocal differences in sympathetic discharge [30]. This explains the hemispheric asymmetry during normal breathing. Furthermore, the significantly higher connectivity in the right hemisphere may be interpreted in the context that all subjects were right-handed. Studies have already reported a correlation between nasal airflow and handedness based on the observation that there is often a consistency in lateral preferences with the dominant nostril positively correlated with the dominant hand [31]. Contrary to normal breathing, during the breath-hold sessions, no statistically significant differences exist between the FC of the left and right brain hemispheres, in the delta and alpha band, as illustrated in Fig. 2. Thus, it may be inferred that, in these EEG bands, breath-hold indeed has a balancing effect on the FC of the left and right brain hemispheres. This is in line with the existing literature which suggests that these bands are highly influenced by hypercapnic stimuli [18], [32].

The Pearson correlation and Spearman Rho between left and right brain hemispheres during normal breathing, exhale-hold, and inhale-hold were computed separately for each EEG band. The significance of the correlation was less than 0.001 for all cases, and both the correlation coefficients gave positive values. The delta EEG band exhibited a maximum Pearson correlation of 0.908, 0.897, and 0.894 between brain hemispheres during normal breathing, inhale-hold, and exhale-hold, respectively. The corresponding Spearman Rho values were 0.846, 0.792, and 0.840 respectively. The difference in

values can be attributed to the fact that Pearson correlation coefficient measures the linear relationship between the variables while Spearman correlation coefficient measures monotonic relationships in which the variables tend to move in the same/opposite direction but not necessarily at a constant rate, whereas the rate is constant in a linear relationship. Also, in the beta band, the Spearman Rho was found to be higher than the Pearson correlation for all three cases, indicating a lesser linear and higher monotonic trend.

Further, differences in FC were analysed in seven cortical regions of the brain during NB, EH, and IH. Analyses were done separately for five specific EEG bands as illustrated in Fig.3. It may be noted that all seven cortical regions exhibit a decreasing trend in the strength of functional connections (indicated by the phase synchronization measure) as the frequency range increases from delta to gamma band.

In the delta band, 5 out of 7 cortical regions showed significant differences in the FC between normal breathing and one or both of breath-hold tasks. Specifically, the central and parietal regions showed differences of comparatively higher statistical significance. This was expected as previous studies have shown that automatic control of breathing, especially those producing hypoxic conditions, can cause respiration-locked oscillations in the somatosensory cortex [10] and parietal cortex [8].

The theta band FC at the parietal region showed significant discriminating capacity between normal breathing and breath-hold. An increased concentration required on behalf of the subject to perform the breath-hold tasks might be responsible for such significant variations in the theta band FC of the parietal area of the brain [33]. This reasoning can also be extended to explain the utility of the alpha-band FC of the parietal region to distinguish between normal breathing and inhale-hold. The alpha band connectivity in the frontal and central regions of the brain also showed discriminating power, although of a lesser significance, between normal breathing and breath-hold. This is in agreement with the existing literature that has reported significant alpha variations in the generic coupling between the brain and respiratory activity in the middle anterior region of the brain during breath-hold [18].

The beta band illustrated statistically significant differences between the FC measures during normal breathing and breath-hold, in the parietal and occipital lobes. The posterior cortex is known to be active during resting states by increasing FC within the brain's default mode network, which involves the precuneus, the posterior cingulate cortex, and the lateral parietal lobe [34]. Moreover, concordant with our observation, Huang and Lo have previously reported increased activity in the occipital beta band in Zen meditation practitioners who regularly practice slow-breathing and breath-hold techniques [35].

Finally, the gamma band demonstrates significant FC variations only in the pre-frontal region of the brain. One interesting observation was the unique ability of the gamma band FC in the pre-frontal region to distinctly identify the inhale-hold and exhale-hold tasks. The findings reveal that the respiratory cycle can modulate high-frequency oscillations such as gamma activity as well, which are known to govern higher cognitive functions like decision making, problem-solving, language processing, and sensory perception. The activations in the pre-frontal region that are implicated for executive functions further strengthen this revelation.

Furthermore, the correlation analyses were done across brain regions, for different EEG bands. The analyses illustrated strongest correlations between frontal-anterior frontal, anterior frontal-prefrontal, and parietal-frontal regions of the brain. While the lower frequency bands (viz., delta, theta, and alpha) showed strong correlations in a shorter range involving pre-frontal, anterior frontal, and frontal regions, the higher frequency bands (viz., beta and gamma) exhibited strong long-range correlations between parietal and frontal regions of the brain.

V. Conclusions

In conclusion, this paper investigates the effect of normal breathing and breath-hold on the FC of the human brain. The observations highlight that the functional connections in the human brain exhibit a hemispherical symmetry during breath-hold in the delta and alpha bands. The study also revealed that during breathing and breath-hold, synchronization of neuronal assemblies in different cortical regions of the brain is higher in the low-frequency EEG bands and lower in the high-frequency EEG bands. Furthermore, the gamma-band functional connections of the pre-frontal cortex could distinctly identify the inhale-hold from exhale-hold. These results may provide interesting clues toward the comprehension of the mechanisms underlying breath control and the extent to which rhythmic brain activity is modulated by the rhythmic act of breathing.

Acknowledgment

The authors thank the Cognitive Science Research Initiative (CSRI) of the Department of Science & Technology, Government of India for funding part of this work under the postdoctoral fellowship grant No. DST/CSRI-PDF/2021/39 to the first author.

References

[1] R. Stevens, A. Plüddemann, and R. I. Maconochie, "Normal ranges of heart rate and respiratory rate in children from birth to 18 years: A systematic review of observational studies," *Lancet*, vol. 377, no. 9770, pp. 1011–1018, Mar. 2011.

[2] J. D. Moore *et al.*, "Hierarchy of orofacial rhythms revealed through whisking and breathing," *Nature*, vol. 497, no. 7448, pp. 205–210, 2013.

[3] L. C. Mckay *et al.*, "Neural correlates of voluntary breathing in humans," *J. Appl. Physiol.*, vol. 95, no. 3, pp. 1170–1178, Sep. 2003.

[4] H. Liu, J. Allen, D. Zheng, and F. Chen, "Recent development of respiratory rate measurement technologies," *Physiol. Meas.*, vol. 40, no. 7, p. 07TR01, Jul. 2019.

[5] S. Shu *et al.*, "Non-contact measurement of human respiration using an infrared thermal camera and the deep learning method," *Meas. Sci. Technol.*, Mar. 2022.

[6] P. Jagadev, S. Naik, and L. I. Giri, "Contactless monitoring of human respiration using infrared thermography and deep learning," *Physiol. Meas.*, vol. 43, no. 2, p. 025006, 2022.

[7] J. E. Butler, "Drive to the human respiratory muscles," *Respir. Physiol. Neurobiol.*, vol. 159, no. 2, pp. 115–126, Nov. 2007.

[8] J. L. Herrero *et al.*, "Breathing above the brain stem: Volitional control and attentional modulation in humans," *J. Neurophysiol.*, vol. 119, no. 1, pp. 145–159, Jan. 2018.

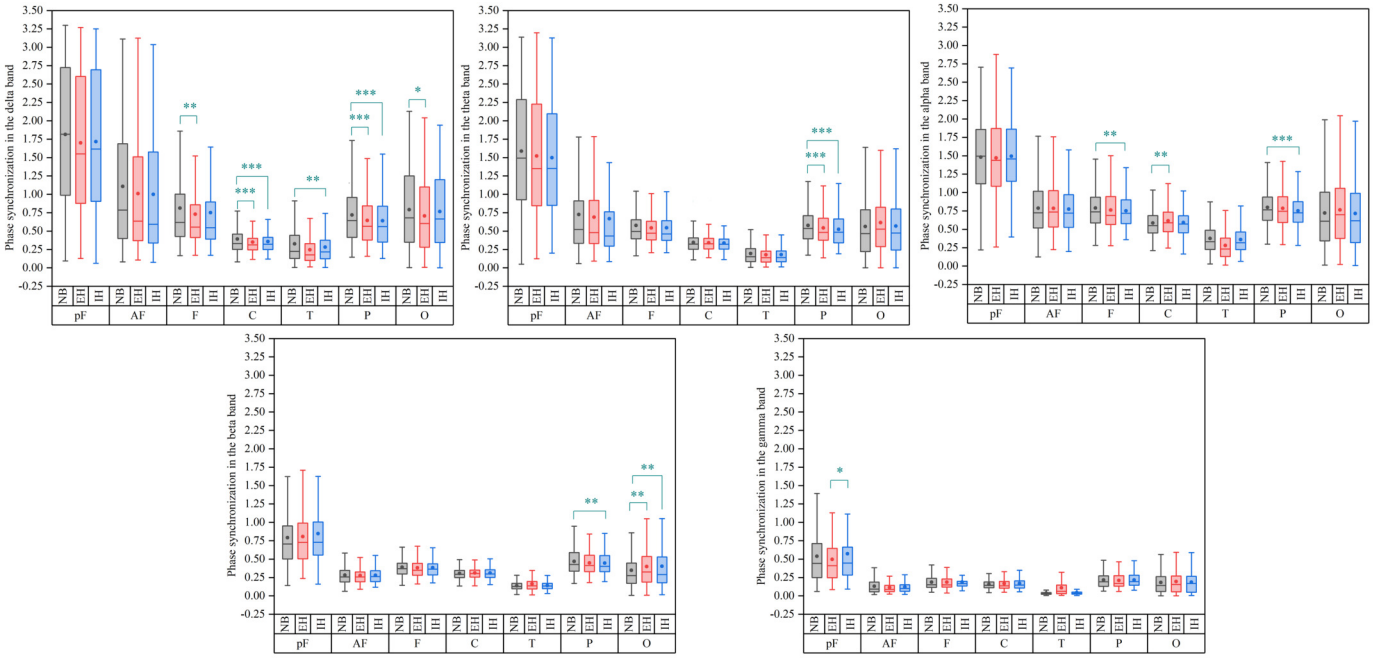

Fig. 3. Grand average of FC estimations in different cortical regions. All cortical regions exhibit a decreasing trend in the strength of functional connections as the frequency range increases from delta to gamma band. Box is determined by the 25th and 75th percentiles. Whiskers indicate 1.5 times the interquartile range (IQR). Circle represents the mean value and dash represents the median value. Representation of significance thershold is as follows: ns is $p > 0.05$, * is $p \leq 0.05$, ** is $p \leq 0.01$, and *** is $p \leq 0.001$.

[9] D. E. Frederick *et al.*, "Gamma and beta oscillations define a sequence of neurocognitive modes present in odor processing," *J. Neurosci.*, vol. 36, no. 29, pp. 7750–7767, 2016.

[10] J. Ito *et al.*, "Whisker barrel cortex delta oscillations and gamma power in the awake mouse are linked to respiration," *Nat. Commun.*, vol. 5, no. 1, pp. 1–10, Apr. 2014.

[11] S. Bagur *et al.*, "Breathing-driven prefrontal oscillations regulate maintenance of conditioned-fear evoked freezing independently of initiation," *Nat. Commun.*, vol. 12, no. 1, pp. 1–15, 2021.

[12] O. Perl *et al.*, "Human non-olfactory cognition phase-locked with inhalation," *Nat. Hum. Behav.*, vol. 3, no. 5, pp. 501–512, 2019.

[13] C. Zelano *et al.*, "Nasal respiration entrains human limbic oscillations and modulates cognitive function," *J. Neurosci.*, vol. 36, no. 49, pp. 12 448–12 467, 2016.

[14] N. Verschoor *et al.*, "The lowering of stroke volume measured by means of impedance cardiography during endexpiratory breath holding," *Physiol. Meas.*, vol. 17, no. 1, p. 29, 1996.

[15] H. Rehouma *et al.*, "Quantitative assessment of spontaneous breathing in children: evaluation of a depth camera system," *IEEE Trans. Instrum. Meas.*, vol. 69, no. 7, pp. 4955–4967, 2019.

[16] E. Williams, N. Bednarczuk, T. Dassios, and A. Greenough, "Factors affecting the arterial to end-tidal carbon dioxide gradient in ventilated neonates," *Physiol. Meas.*, vol. 43, no. 2, p. 025005, 2022.

[17] M. S. Morelli *et al.*, "A cross-correlational analysis between electroencephalographic and end-tidal carbon dioxide signals: Methodological issues in the presence of missing data and real data results," *Sensors*, vol. 16, no. 11, p. 1828, 2016.

[18] ——, "Analysis of generic coupling between EEG activity and $P_{ET}CO_2$ in free breathing and breath-hold tasks using Maximal Information Coefficient (MIC)," *Sci. Rep.*, vol. 8, no. 1, p. 4492, Mar. 2018.

[19] A. G. Ramakrishnan, A. Adarsh, K. Sharma, and K. G. Pradeep, "Anomaly in respiratory sinus arrhythmia–multiple heart rate variability cycles within each breathing cycle at low breath rates with breath holds," in *IEEE Int. Conf. on Electronics, Computing and Communication Technologies (CONECCT)*, 2020, pp. 1–6.

[20] A. G. Ramakrishnan and A. Adarsh, "R-wave amplitude changes and atypical heart rate changes accompanying breath hold during low breathing rates," in *42nd Annu. Int. Conf. of the IEEE Engineering in Medicine and Biology Society (EMBC)*, 2020, pp. 2667–2670.

[21] A. C. Zappe *et al.*, "The influence of moderate hypercapnia on neural activity in the anesthetized nonhuman primate," *Cerebral Cortex*, vol. 18, no. 11, pp. 2666–2673, 2008.

[22] M. Jones *et al.*, "The effect of hypercapnia on the neural and hemodynamic responses to somatosensory stimulation," *Neuroimage*, vol. 27, no. 3, pp. 609–623, 2005.

[23] F. Matakas, J. Birkle, and J. Cervós-Navarro, "The effect of prolonged experimental hypercapnia on the brain," *Acta Neuropathol.*, vol. 41, no. 3, pp. 207–210, 1978.

[24] T. Zhang *et al.*, "Regional characterization of functional connectivity in patients with sleep apnea hypopnea syndrome during sleep," *Physiol. Meas.*, vol. 42, no. 7, p. 075004, 2021.

[25] N. Kanwisher, "Functional specificity in the human brain: A window into the functional architecture of the mind," *Proc. Natl. Acad. Sci.*, vol. 107, no. 25, pp. 11 163–11 170, 2010.

[26] K. J. Friston, "Functional and effective connectivity in neuroimaging: A synthesis," *Hum. Brain Mapp.*, vol. 2, no. 1-2, pp. 56–78, 1994.

[27] http://mile.ee.iisc.ac.in/downloads.html.

[28] C. Brunner, A. Delorme, and S. Makeig, "EEGLAB - An open source matlab toolbox for electrophysiological research," *Biomed. Eng.*, vol. 58, no. SI-1-Track-G, p. 000010151520134182, 2013.

[29] R. Eccles and R. L. Lee, "The influence of the hypothalamus on the sympathetic innervation of the nasal vasculature of the cat," *Acta Oto-Laryngol.*, vol. 91, no. 1-6, pp. 127–134, Jan. 1981.

[30] A. Price and R. Eccles, "Nasal airflow and brain activity: Is there a link?" *J. Laryngol. Otol.*, vol. 130, no. 9, pp. 794–799, Sep. 2016.

[31] A. Searleman *et al.*, "Nostril dominance: Differences in nasal airflow and preferred handedness," *Laterality: Asymmetries of Body, Brain and Cognition*, vol. 10, no. 2, pp. 111–120, Mar. 2005.

[32] D. Wang *et al.*, "Comparing the effect of hypercapnia and hypoxia on the electroencephalogram during wakefulness," *Clin. Neurophysiol.*, vol. 126, no. 1, pp. 103–109, Jan. 2015.

[33] Y. Kubota *et al.*, "Frontal midline theta rhythm is correlated with cardiac autonomic activities during the performance of an attention demanding meditation procedure," *Cogn. Brain Res.*, vol. 11, no. 2, pp. 281–287, 2001.

[34] M. E. Raichle, "The brain's default mode network," *Annu. Rev. Neurosci.*, vol. 38, pp. 433–447, Jul. 2015.

[35] H. Y. Huang and P. C. Lo, "EEG dynamics of experienced Zen meditation practitioners probed by complexity index and spectral measure," *J. Med. Eng. Technol.*, vol. 33, no. 4, pp. 314–321, 2009.